

A major purpose of the Technical Information Center is to provide the broadest dissemination possible of information contained in DOE's Research and Development Reports to business, industry, the academic community, and federal, state and local governments.

Although a small portion of this report is not reproducible, it is being made available to expedite the availability of information on the research discussed herein.

**1**

NOTICE  
PORTIONS OF THIS REPORT ARE ILLISIBLE.  
It has been reproduced from the best  
available copy to permit the broadest  
possible availability.

Los Alamos National Laboratory is operated by the University of California for the United States Department of Energy under contract W-7405-ENG-36

LA-UR--84-2752

DESG 015821

TITLE THE THREE-DIMENSIONAL HYDRODYNAMIC HOT-SPOT

AUTHOR(S) C. L. Mader, T-14

SUBMITTED TO Paul Vieille Scientific Meeting, September 26-27, 1984,  
Vert-le-Petit, France

MASTER

DISCLAIMER

This report was prepared as an account of work sponsored by an agency of the United States Government. Neither the United States Government nor any agency thereof, nor any of their employees, makes any warranty, express or implied, or assumes any legal liability or responsibility for the accuracy, completeness, or usefulness of any information, apparatus, product, or process disclosed, or represents that its use would not infringe privately owned rights. Reference herein to any specific commercial product, process, or service by trade name, trade mark, manufacturer, or otherwise does not necessarily constitute or imply its endorsement, recommendation, or favoring by the United States Government or any agency thereof. The views and opinions of authors expressed herein do not necessarily state or reflect those of the United States Government or any agency thereof.

By acceptance of this article the publisher recognizes that the U.S. Government retains a nonexclusive, royalty-free license to publish or reproduce the published form of this contribution or to allow others to do so, for U.S. Government purposes.

The Los Alamos National Laboratory requests that the publisher identify this article as work performed under the auspices of the U.S. Department of Energy.

Los Alamos Los Alamos National Laboratory  
Los Alamos, New Mexico 87545

# THE THREE-DIMENSIONAL HYDRODYNAMIC HOT-SPOT

by

Charles L. Mader

Los Alamos National Laboratory  
Los Alamos, New Mexico 87545 (USA)

## ABSTRACT

The basic processes in the shock initiation of heterogeneous explosives have been investigated theoretically using a model of a cube of nitromethane containing 91 cubic air holes. The interaction of a shock wave with a single air hole and a matrix of air holes in PETN, HMX, and TATB has been numerically modeled. The interaction of a shock wave with the density discontinuities, the resulting hot-spot formation and interaction, and the buildup to propagating detonation were computed using three-dimensional numerical Eulerian hydrodynamics with Arrhenius chemical reaction and accurate equations of state according to the hydrodynamic hot-spot model. The basic processes in the desensitization of a heterogeneous explosive by preshocking with a shock pressure too low to cause propagating detonation was numerically modeled. The basic differences between shock sensitive explosives such as PETN or HMX and shock insensitive explosives such as TATB or NQ may be described using the hydrodynamic hot-spot model.

---

## I. INTRODUCTION

The hydrodynamic stability of one-dimensional detonations in an ideal gas of constant heat capacity undergoing an exothermic, irreversible, unimolecular reaction with an Arrhenius-law temperature dependence has been studied analytically by Erpenbeck.<sup>1</sup> The analysis gives no information about the nature of the time-dependent behavior of the flow for finite perturbations (the stability) of the ideal gas reaction zone using a one-dimensional characteristic method. In those cases for which Erpenbeck's linearized analysis has shown the steady-

state solution to be unstable to infinitesimal longitudinal perturbations, flows started in a configuration approximating the steady-state solution exhibited nondecaying oscillations; in those cases for which Erpenbeck's analysis showed the steady-state solution to be stable, perturbations were found to decay.<sup>2</sup>

In Ref. 3 we described the results of our studies of the time-dependent behavior of the flow (the stability) of the ideal gas, nitromethane, and liquid TNT reaction zones to finite longitudinal and transverse perturbations using finite difference methods to solve the reactive Navier-Stokes equations of fluid dynamics. We also described the time-dependent behavior of the flow of stable overdriven nitromethane detonations formed by pistons of various configuration.

The constant velocity piston calculations with a resolved reaction zone show details of the process of shock initiation of nitromethane. The basic features are identical to those of the flow computed with an unresolved reaction zone.<sup>4</sup> The shocked nitromethane first completely decomposes at the piston and achieves a detonation with a peak pressure that builds up toward the C-J pressure of the high density shocked nitromethane. The detonation overtakes the shock wave and the pressure at the end of the reaction zone decays toward the piston pressure.

If one introduces gas bubbles or grit into a homogeneous explosive such as a liquid or a single crystal, thereby producing a heterogeneous explosive, the minimum shock pressure necessary to initiate propagating detonation can be decreased by one order of magnitude.

Heterogeneous explosives, such as PBX-9404 or PBX-9502, show a different behavior than homogeneous explosives when propagating along confining surfaces. A heterogeneous explosive can turn sharp corners and propagate outward, and depending upon its sensitivity, it may show either very little or much curvature when propagating along a metal surface. The mechanism of initiation for heterogeneous explosives is different than the simple Arrhenius kinetic model found adequate for homogeneous explosives. Heterogeneous explosives are initiated and may propagate by the process of shock interaction with density discontinuities such as voids. These interactions result in hot regions that decompose and produce increasing pressures that cause more and

hotter decomposing regions. The shock wave increases in strength, releasing more and more energy, unless it becomes strong enough that all of the explosive reacts and detonation begins.

This process is described by the "hydrodynamic hot-spot model, which models the hot-spot formation from the shock interactions that occur at density discontinuities and describes the decomposition using the Arrhenius rate law and the temperature from the HOM equation of state.<sup>5</sup>

The numerical modeling of the interaction of a shock wave with a single density discontinuity was reported in Ref. 5 where an 8.5-GPa shock interacting with a single spherical hole in nitromethane was studied. The study was extended to four rectangular holes<sup>5</sup> where it was determined that a 0.0032-mm-radius cylindrical void would initiate propagating detonation and a 0.001-mm-radius void would form a hot spot which failed to propagate because of rarefactions cooling the reactive wave.

We have studied the buildup of an 8.5-GPa shock wave in nitromethane as it interacts with 91 cubes, 0.002 mm or 0.0004 mm on a side. The cubes simulate a random spacing.

It has been observed that preshocking a heterogeneous explosive with a shock pressure too low to cause propagating detonation in the time of interest can cause a propagating detonation in unshocked explosive to fail to continue propagating when the detonation front arrives at the previously shocked explosive. For explosives that have been previously shocked, it has been experimentally observed<sup>6</sup> that the distance of run to detonation for several multiple-shocked explosives is determined primarily by the distance after the second shock has overtaken the lower pressure shock wave (the preshock). In this study we examine the basic process in the desensitization of heterogeneous explosives by preshocking.

When a shock wave interacts with a hole, a hot spot with temperatures several hundred degrees hotter than the surrounding explosive is formed in the region above the hole when it is collapsed by the shock wave. The hot region decomposes and contributes energy to the shock wave, which has been degraded by the hole interaction.

Whether this energy is sufficient to compensate for the loss from the hole interaction depends upon the magnitude of the initial shock wave, the hole size, and the interaction with the flow from nearest neighbor hot spots. The objective of the study was to investigate the nature of this complicated interaction and to determine if the hydrodynamic hot-spot model was adequate to describe the experimentally observed sensitivity to shock initiation of the heterogeneous explosives PETN, HMX, TATB, and Nitroguanidine with PETN being the most sensitive and Nitroguanidine the least sensitive.

## II. NUMERICAL MODELING

The three-dimensional Eulerian reactive hydrodynamic code 3DE is described in Ref. 7. It uses techniques identical to those described in detail in Ref. 5 and used successfully for describing two-dimensional Eulerian flow with mixed cells and multicomponent equations of state, and for modeling reactive flow.

The three-dimensional code has been used to study the interaction of two, three, and five colliding, diverging spherical detonation waves in PBX-9404. As described in Ref. 8, the size and magnitude of the high-pressure double, triple, quadruple, and quintuple interactions depend upon the number and relative location of the initiators. The initiation of propagating detonation in the insensitive explosive PBX-9502 by triple shock wave interaction resulting from three initiators has also been studied. The reactive hydrodynamics of a matrix of tungsten particles in HMX was described in Ref. 9.

The Arrhenius reactive rate law was used with the constants determined experimentally by Raymond N. Rogers and described in Refs. 5, 6, and 10.

The HOM equation of state constants used for nitromethane and PETN are described in Ref. 5. The BKW detonation product and the solid equation of state constants used in the HOM equation of state for HMX, TATB, and Nitroguanidine (NQ) are given in Ref. 10.

A constant velocity piston was applied to the bottom of the explosive cube, shocking the explosive initially to the desired pressure.

### III. NITROMETHANE NUMERICAL RESULTS

To determine the effect of numerical resolution on critical details of the hot-spot temperature gradients, calculations were performed with various resolution for the interaction of an 8.5-GPa shock in nitromethane with a single 0.002-mm cubical hole. The results were compared with the two-dimensional calculations for a 0.002-mm cylindrical hole described in Ref. 5. Similar results were obtained for the cubical hole resolved with 5, 4, and 3 cells along a side or 125, 64, and 27 cells per hole. However, two cells along a side or eight cells per hole resulted in the temperature gradient of the hot spot being too smeared. Because the calculations were long and expensive, we wished to use the lowest resolution possible to study the basic processes involved. It was determined<sup>6</sup> that increasing the frequency factor would compensate for the effects of low resolution of the hot spot, so most of the calculations were performed with low resolution and the compensating frequency factor. During the total time of interest in the calculation, the bulk of the nitromethane is essentially undecomposed and the pressure remains constant behind the shock wave in the unperturbed regions of the flow.

The interaction of an 8.5-GPa shock in a 0.028-mm cube of nitromethane with ninety-one 0.002-mm cubical holes (Fig. 1) and chemical reaction is shown in Fig. 2. The shock interacts with the first layer of holes causing hot spots upon closure of the holes, which decompose but do not result in propagating detonation in the remainder of the nitromethane. The decomposition enhances the shock wave so that, upon interaction with upper voids, hotter and larger hot spots are formed and result in shocks sufficiently strong to build toward propagating detonation. Similar results were obtained from a high resolution calculation of this problem.

The interaction of an 8.5-GPa shock in a 0.0056-mm cube of nitromethane with ninety-one 0.0004-mm cubical holes and chemical reaction is shown in Fig. 3. The problem is identical to that of Fig. 2, except scaled by 0.2.

The hot spots form, but are so small that they are quickly cooled by the side and rear rarefactions before they can decompose enough to

significantly enhance the shock wave. The hot spots continue to react slowly and keep the pressure behind the shock front from decaying. This slow decomposition was observed<sup>5</sup> in the shock initiation of heterogeneous explosives when an explosive continued to decompose behind the shock front and even after the shock wave passed through a slab of explosive too thin to build to propagating detonation.

The interaction of a 5.5-GPa, 1.72-g/cm<sup>3</sup>, shock generated by a constant velocity piston moving at 1.29 mm/ $\mu$ s in a 0.028-mm cube of nitromethane with ninety-one 0.002-mm cubical holes and chemical reaction is shown in Fig. 4. The resulting hot spots are too cool (less than 900 K) to cause appreciable decomposition before the side and rear rarefactions further reduce the temperature of the hot spot.

The interaction of a 5.5-GPa shock for 0.0016  $\mu$ s followed by an 8.5-GPa shock in a 0.028-mm cube of nitromethane with ninety-one 0.002-mm cubical holes is shown in Fig. 5. The 5.5-GPa shock wave closes the holes and makes low-temperature hot spots, which result in very little decomposition of the explosive. The following 8.5-GPa shock wave does not have holes with which to interact. The precompressed nitromethane resembles a homogeneous explosive with the second shock causing only some additional bulk shock heating. The multiple shocking also results in a lower nitromethane shock temperature than if it had been singly shocked to 8.5 GPa.

When the 8.5-GPa shock wave catches up with the 5.5-GPa shock wave, it then interacts with the remaining holes, forming hot spots which decompose and support the shock wave growth building toward a propagating detonation. This models the experimentally observed behavior of the distance of run to detonation for multiple shocked explosives being determined primarily by the distance after the second shock has overtaken the preshock.

#### IV. HMX, PETN, TATB, AND NQ NUMERICAL RESULTS

To initiate PBX-9404 (HMX-based explosive) or PBX-9502 (TATB-based explosive) at maximum pressed density within 4 mm of shock run requires a shock wave in PBX-9404 of 5 GPa and in PBX-9502 of 16 GPa as determined from the experimental Pop plots.<sup>11</sup>



To initiate PETN at  $1.75 \text{ g/cm}^3$  (crystal density is 1.778) within 4 mm of shock run requires a pressure of only 2 GPa, while to initiate Nitroguanidine at  $1.723 \text{ g/cm}^3$  (crystal density is 1.774) within 4 mm of shock run requires a pressure of 25 GPa.<sup>11</sup>

The hole size present in such pressed explosives varies from holes of 20 to 600 Å in the TATB crystals to holes as large as 0.5 mm in the explosive-binder matrix. Most of the holes vary in size from 0.05 to 0.005 mm in diameter, so we examined holes in that range of diameters.

As shown in Ref. 5, the hot spot formed when a shock wave interacts with a spherical hole scales with the radius of the hole as long as no chemical reaction occurs. Using hot-spot temperatures in the calculated range of 700 to 1300 K and calculating the adiabatic explosion shown in Table I. The ordering is identical to that observed experimentally.

The interaction of shock waves of various pressures with single cubical air holes of various sizes in PETN, HMX, TATB, and NQ was investigated. The calculations model the hot-spot explosion and failure to propagate because of rarefactions cooling the reactive wave. If the reaction becomes too fast to numerically resolve the cooling by rarefactions, the flow builds toward a detonation too quickly.

TABLE I. Adiabatic Explosion Times

Explosive	Hot-Spot Temperature		
	700 K	1000 K	1300 K
Nitroguanidine	5504 $\mu\text{s}$	124 $\mu\text{s}$	18.47 $\mu\text{s}$
TATB	1290 $\mu\text{s}$	$6 \times 10^{-3} \mu\text{s}$	$1 \times 10^{-5} \mu\text{s}$
HMX	5.26 $\mu\text{s}$	$1 \times 10^{-4} \mu\text{s}$	$5 \times 10^{-7} \mu\text{s}$
PETN	0.08 $\mu\text{s}$	$7 \times 10^{-6} \mu\text{s}$	$5 \times 10^{-8} \mu\text{s}$

A summary of the results of the study is shown in Table II. The ordering of shock sensitivity of the explosives is again observed experimentally correlating well with the observed Pop plot data.<sup>11</sup>

TABLE II. Single Cubical Air-Hole Study

Explosive	Air Cube Size (mm)	Pressure (GPa)	Result
HMX	$5 \times 10^{-3}$	2.5	Fails to build toward a detonation
	$5 \times 10^{-3}$	5.0	Fails to build toward a detonation
	$5 \times 10^{-3}$	7.5	Builds toward a detonation
	$5 \times 10^{-2}$	2.5	Fails to build toward a detonation
	$5 \times 10^{-2}$	5.0	Marginal
	$5 \times 10^{-2}$	7.5	Builds toward a detonation
TATB	$5 \times 10^{-3}$	5.0	Fails
	$5 \times 10^{-3}$	12.5	Fails
	$5 \times 10^{-3}$	15.0	Builds toward a detonation
	$5 \times 10^{-2}$	7.5	Fails
PETN	$5 \times 10^{-3}$	2.5	Builds toward a detonation
	$5 \times 10^{-3}$	7.5	Builds toward a detonation
Nitroguanidine	$5 \times 10^{-2}$	25.0	Fails
	5.0	25.0	Builds toward a detonation

To evaluate the sensitivity to shock more realistically, we studied the interaction of a 5-GPa shock wave in HMX with a matrix of spherical holes of  $4 \times 10^{-3}$ -mm diameter. The void fraction is 10%. While a single hole fails to build toward a detonation as shown in Fig. 6, the matrix of holes builds toward a detonation as shown in Fig. 7. The experimental run to detonation for a 5-GPa shock wave in  $1.71 \text{ g/cm}^3$  HMX is 0.17 cm. While a propagating detonation would not be expected to occur experimentally in this geometry (the computed detonation is the result of insufficient numerical resolution to resolve the reaction at high pressures and temperature), the enhancement of the shock wave would occur.

The interaction of a 12.5-GPa shock wave in TATB with a single spherical hole of  $4 \times 10^{-3}$ -mm diameter is shown in Fig. 8. It fails to build toward a detonation. The interaction of a 12.5-GPa shock wave in TATB with a matrix of spherical holes of  $4 \times 10^{-3}$ -mm diameter with a void fraction of 10% is shown in Fig. 9. The flow builds toward a detonation. The experimental run to detonation for a 12.5-GPa shock wave in  $1.71 \text{ g/cm}^3$  TATB is 0.30 cm. The computed detonation occurs too quickly because of insufficient numerical resolution when the shock wave is enhanced to high enough pressures and temperatures by the interacting hot spots.

The interaction of a 2.0-GPa shock wave in PETN with a single spherical hole of  $4 \times 10^{-3}$ -mm diameter is shown in Fig. 10. Build up toward a detonation did not occur. The interaction of a 2.0-GPa shock wave in PETN with a matrix of spherical holes of  $4 \times 10^{-3}$ -mm diameter with a void fraction of 10% is shown in Fig. 11. The flow builds towards a detonation after the hot spots interact. The computed detonation in this geometry is a result of insufficient numerical resolution at high decomposition rates. The experimental run to detonation for a 2.0-GPa shock wave in  $1.60 \text{ g/cm}^3$  PETN is 0.20 cm.

The experimental run to detonation values are about the same for a 12.5-GPa shock wave interacting with TATB with 10% voids, for a 5.0-GPa shock wave interacting with HMX with 10% voids, and for a 2.0 GPa shock wave interacting with PETN with 10% voids.

The computational grid contained  $24 \times 22$  by 36 cells, each  $1 \times 10^{-3}$  mm on a side. The 36 air holes were described by 4 cells per

sphere diameter. Numerical tests with 2 to 6 cells per sphere diameter showed the results were independent of grid size for more than 3 cells per sphere diameter. The air holes were located on a hexagonal close-packed lattice (HCP). The closest distance for the HCP matrix between holes was  $3.8 \times 10^{-3}$  mm. The time step was  $1.0 \times 10^{-5}$   $\mu$ s.

### III. CONCLUSIONS

The hydrodynamic hot-spot model describes the basic difference between shock sensitive and shock insensitive explosives. The interaction of a shock wave with air holes in PETN, HMX, TATB, and NQ, the resulting hot-spot formation, interaction, and the build up toward detonation or failure have been modeled. Increased hole size results in larger hot spots that decompose more of the explosive and add their energy to the shock wave and result in increased sensitivity of the explosive to shock. Increased number of holes also causes more hot spots that decompose more explosive and increase the sensitivity of the explosive to shock. The interaction between hole size and number of holes is complicated and requires numerical modeling for adequate evaluation of specific cases. The hole size can become sufficiently small (the critical hole size) that the hot spot is cooled by side rarefactions before appreciable decomposition can occur. Since increasing the number of holes while holding the percentage of voids present constant results in smaller holes, we have competing processes that may result in either a more or less shock sensitive explosive. If the hole size is below the critical hole size, then the explosive will become less sensitive with increasing number of holes of decreasing diameter.

To evaluate the potential shock sensitivity of an explosive for engineering purposes, one needs to determine experimentally the Arrhenius constants. One then calculates the adiabatic explosion times for several assumed hot-spot temperatures to determine the relative sensitivity of the explosive compared with explosives of known sensitivity. A more detailed evaluation can be obtained from calculations using the hydrodynamic hot-spot model.

The process of shock initiation of heterogeneous explosives has also been investigated numerically by studying the interaction of

shock waves with a cube of nitromethane with 91 holes. An 8.5-GPa shock interacting with 0.002-mm holes did build toward a propagating detonation. The enhancement of the shock wave by the chemical reaction resulting from the hot spots caused by the shock interaction with the first layer of holes resulted in hotter and larger hot spots on each subsequent interaction until the shock wave became strong enough to build toward a propagating detonation. Reducing the size of the holes to 0.0004 mm resulted in a sufficient amount of the explosive decomposing to compensate for the loss in energy to the flow caused by the interaction of the shock wave with the holes. The shock wave slowly grew stronger.

A 5.5-GPa shock wave resulted in insufficient heating of the resulting hot spots to cause significant decomposition.

The basic process of desensitization by preshocking is a result of the holes being closed by the low-pressure initial shock wave without resulting in appreciable explosive decomposition. The higher pressure shock that arrives later does not have holes with which to interact and behaves like a shock wave in a homogeneous explosive until it catches up with the lower pressure preshock wave.

The basic processes in the shock initiation of heterogeneous explosives have been numerically modeled in three dimensions using the hydrodynamic hot-spot model. The interaction of a shock wave with density discontinuities, the resulting hot-spot formation and interaction, and the buildup toward propagating detonation or failure have been modeled.

## REFERENCES

1. J. J. Erpenbeck, *Phys. Fluids* 4, 481 (1961); 5, 604 (1962); 7, 684, 1424 (1964); 8, 1192 (1965); and 9, 1293 (1966).
2. W. Fickett and W. W. Wood, *Phys. Fluids* 9, 903 (1966).
3. Charles L. Mader, "One- and Two-Dimensional Flow Calculation of Reaction Zones of Ideal Gas, Nitromethane, and Liquid TNT Detonation," Twelfth Symposium (International) on Combustion, Williams and Wilkins, 1968, p. 701.
4. Charles L. Mader, *Phys. Fluids* 6, 375 (1963).
5. Charles L. Mader, Numerical Modeling of Detonations, University of California Press (1979).
6. Charles L. Mader and James D. Kershner, "Three-Dimensional Modeling of Shock Initiation of Heterogeneous Explosives," Nineteenth Symposium (International) on Combustion, Williams and Wilkins, 1982, p. 685.
7. Charles L. Mader and James D. Kershner, "Three-Dimensional Eulerian Calculation of Triple-Wave Initiated PBX 9404," Los Alamos Scientific Laboratory report LA-8206 (1980).
8. Charles L. Mader, "Detonation Wave Interactions," Seventh Symposium (International) on Detonation, NSWC MP82-334, 1981, p. 669.
9. Charles L. Mader, James D. Kershner, and George H. Pimbley, *J. Energetic Material* 1, 293 (1984).
10. Charles L. Mader and James D. Kershner, "The Three-Dimensional Hydrodynamic Hot-Spot Applied to PETN, HMX, TATB, and NQ," Los Alamos National Laboratory Report LA-10203-MS (1984).
11. Terry R. Gibbs and Alphonse Popolato, *LASL Explosive Property Data*, University of California Press (1980).

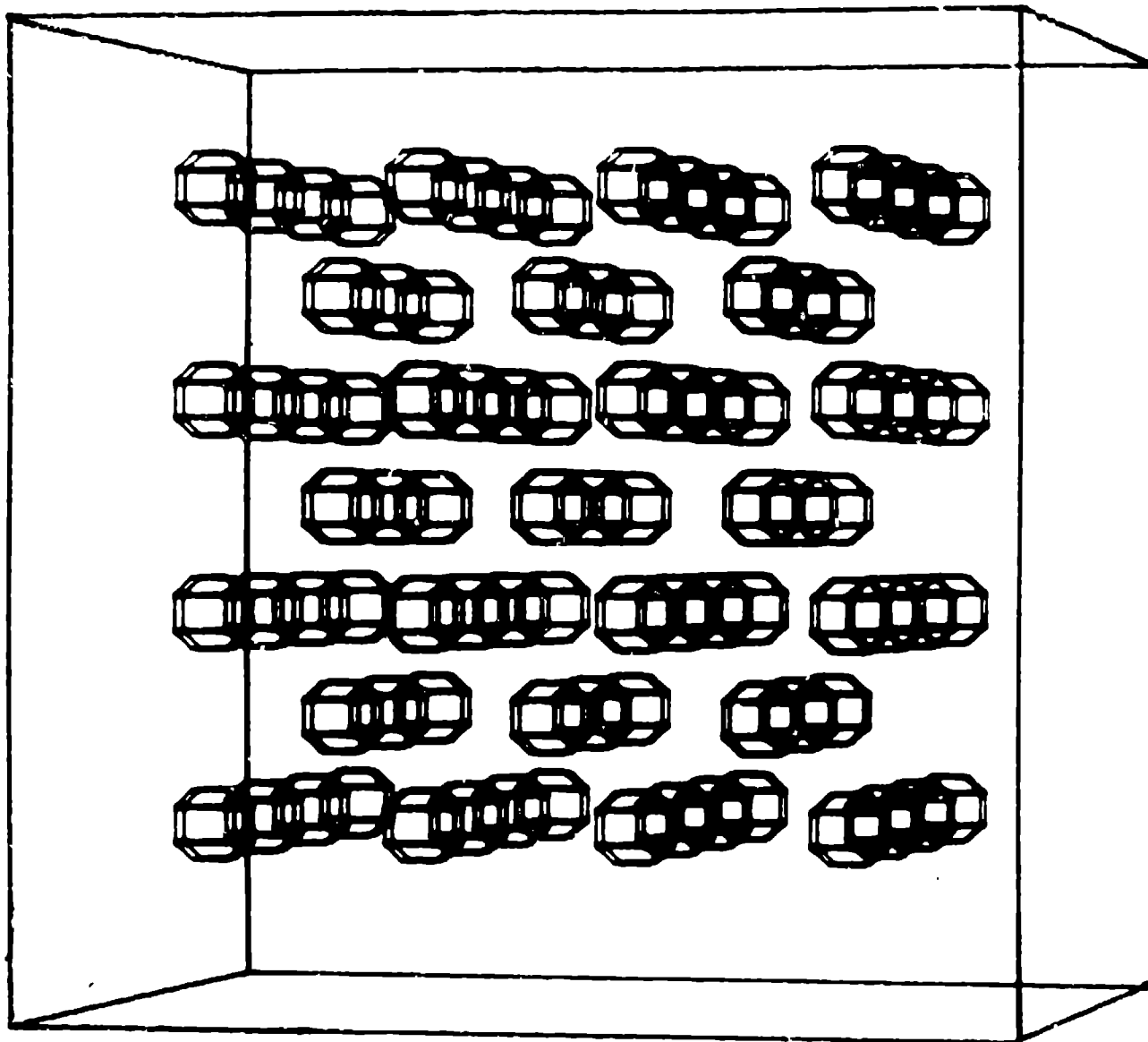


Fig. 1 The initial configuration of 91 cubical air holes in a cube of nitromethane.

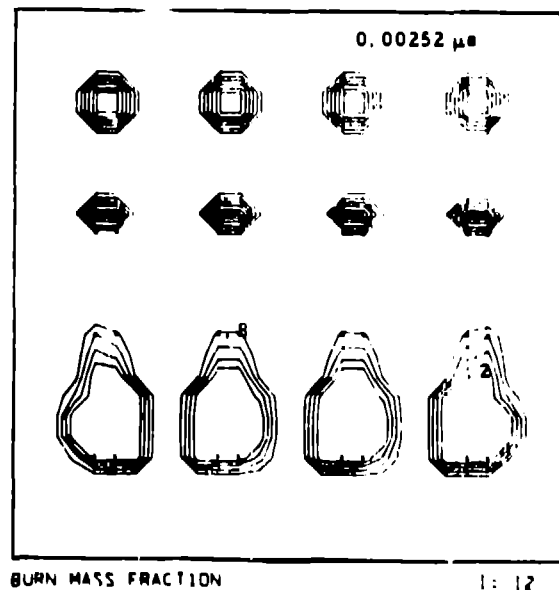
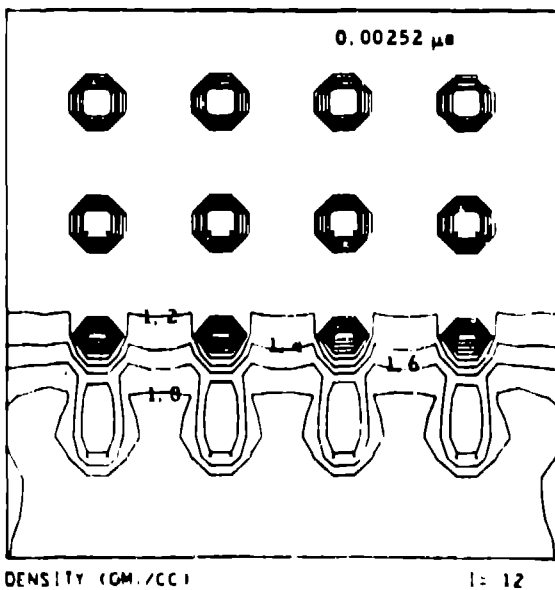
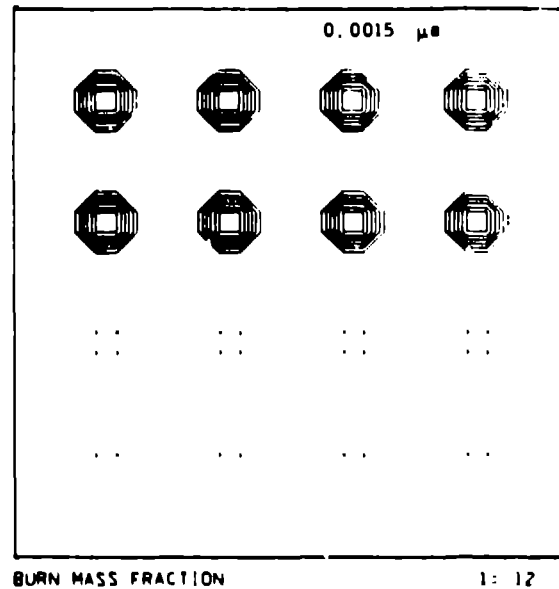
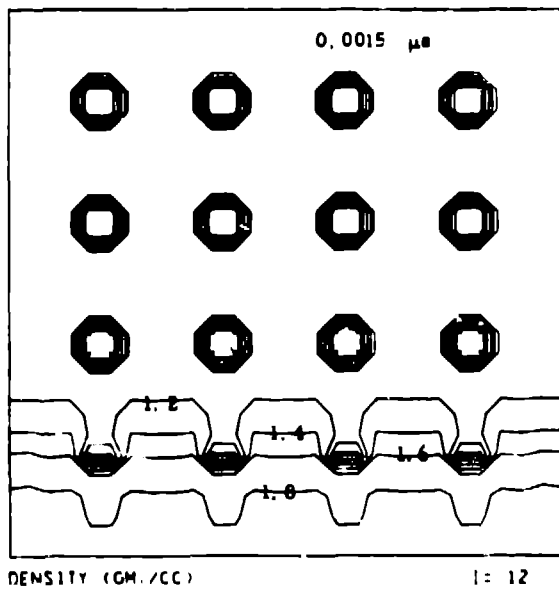
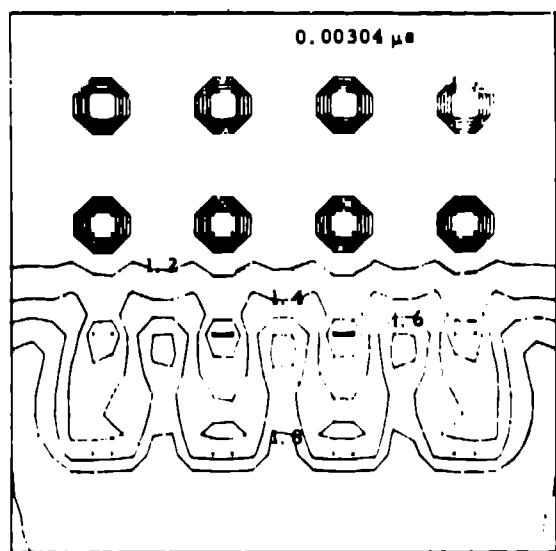


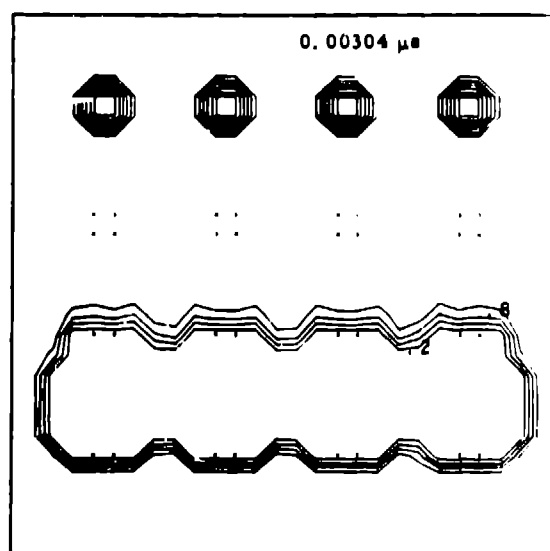
Fig. 2. The cross sections for the 12th cell in the x-direction for the interaction of an 8.5-GPa shock in a 0.028-mm cube of nitromethane with ninety-one 0.002-mm cubical holes. The interval between isopycnics is  $0.2 \text{ mg/mm}^3$  and between burn fraction is 0.2. Shows build-up toward propagating detonation. The lack of symmetry in the center of the calculation is a result of graphic processing and at the sides of the calculation is caused by the boundaries.





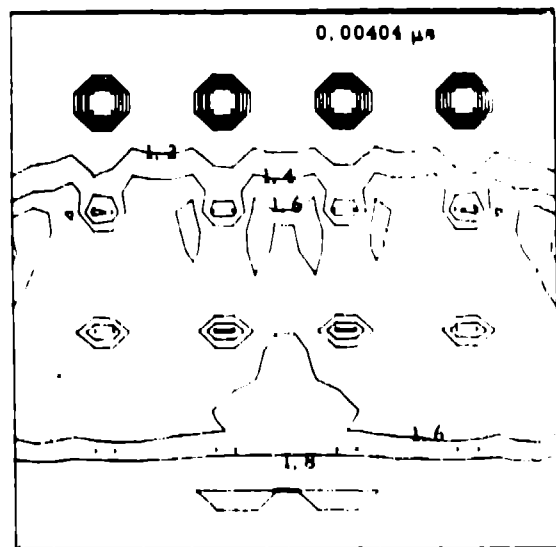
DENSITY (GM./CC)

1: 12



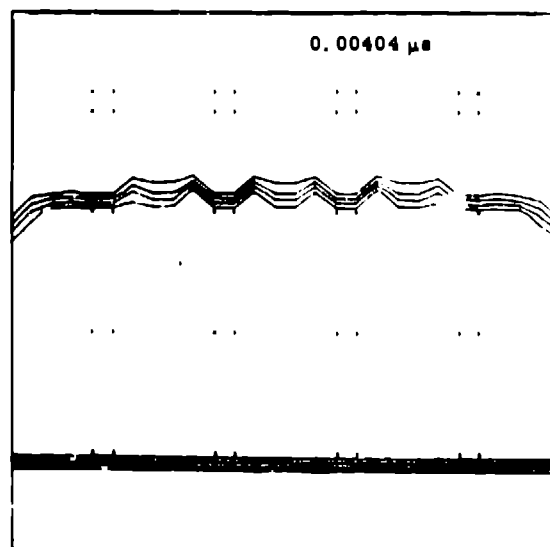
BURN MASS FRACTION

1: 12



DENSITY (GM./CC)

1: 12



BURN MASS FRACTION

1: 12

Fig. 2. (cont)

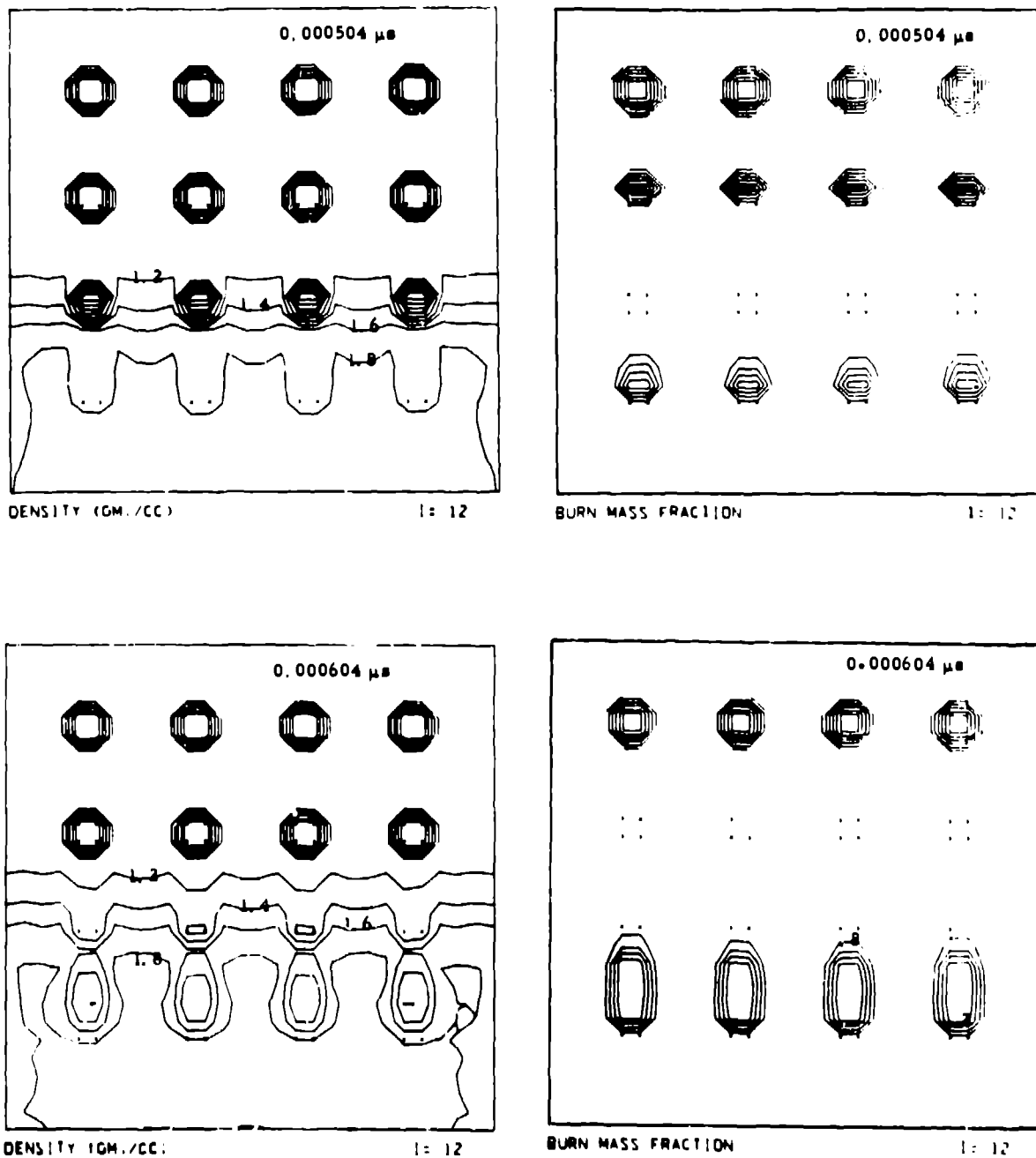


Fig. 3. The cross sections for the 12th cell in the x-direction for the interaction of an 8.5-GPa shock in a 0.0056-mm cube of nitromethane with ninety-one 0.0004-mm cubical holes. The interval between isopycnics is  $0.2 \text{ mg/mm}^3$  and between burn fraction is 0.2. Shows the effect of hole size.

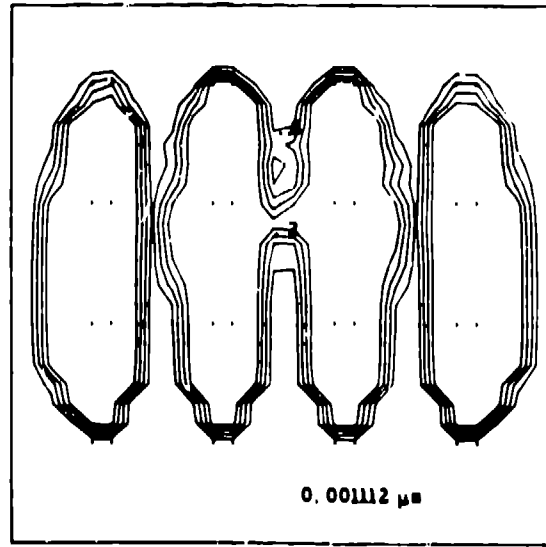
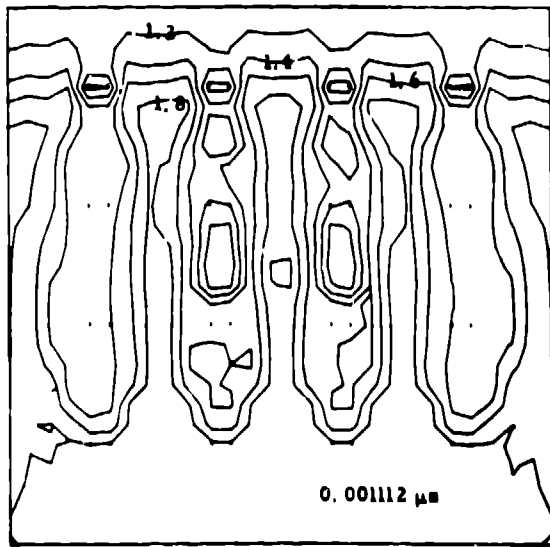
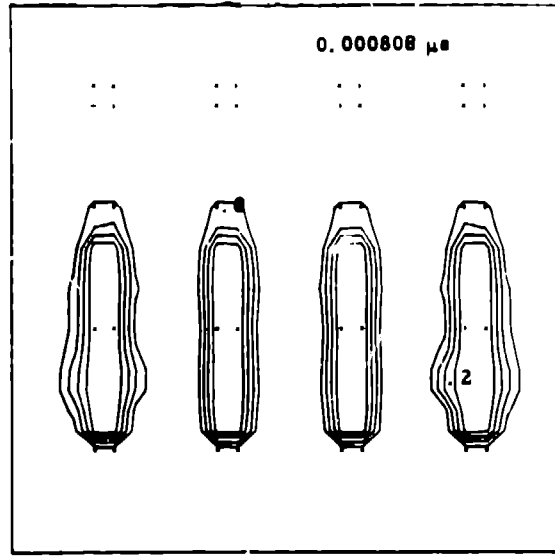
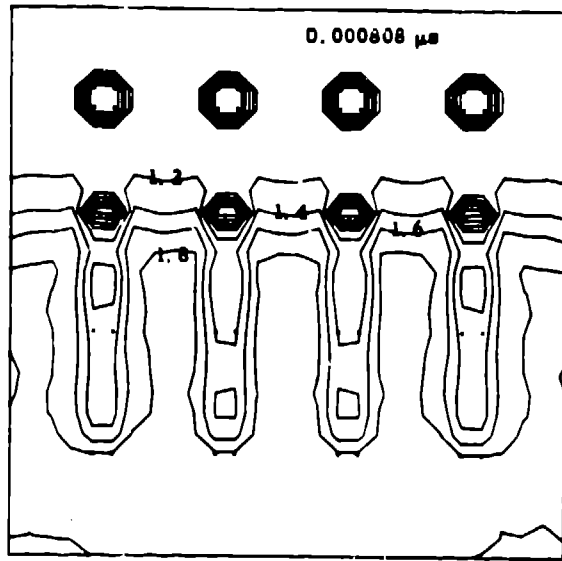


Fig. 3 (cont)

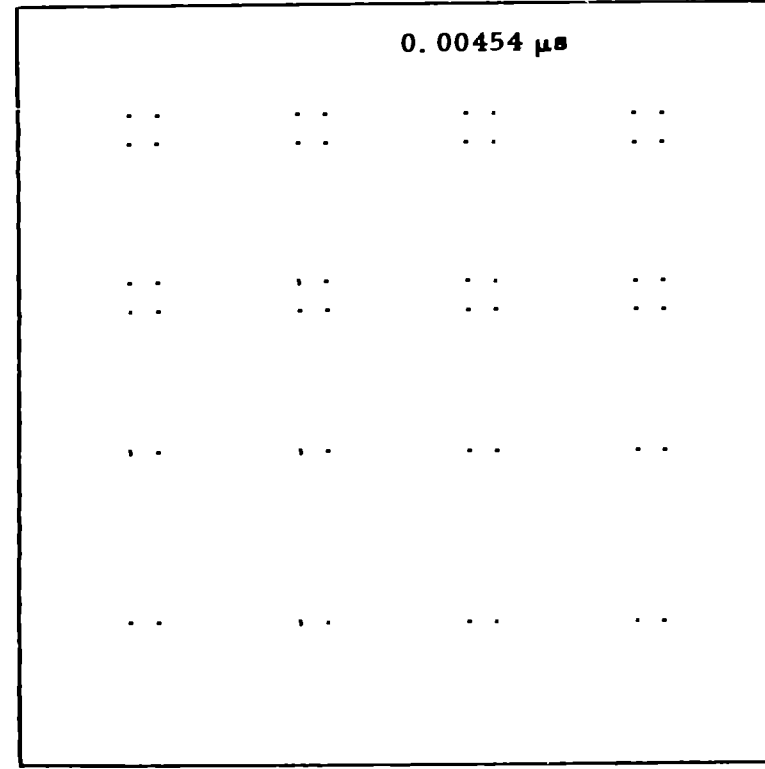
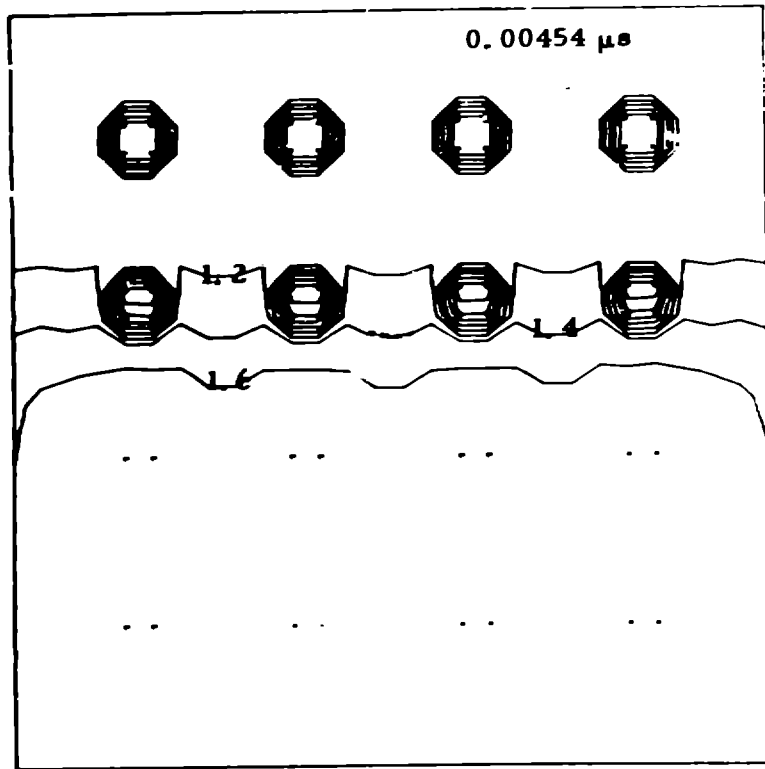


Fig. 4. The cross sections for the 12th cell in the x-direction for the interaction of a 5.5-GPa shock in a 0.028-mm cube of nitromethane with ninety-one 0.002-mm cubical holes. The interval between isopycnics is 0.2 mg/mm<sup>3</sup> and between burn fraction is 0.2. Shows the effect of initial pressure.

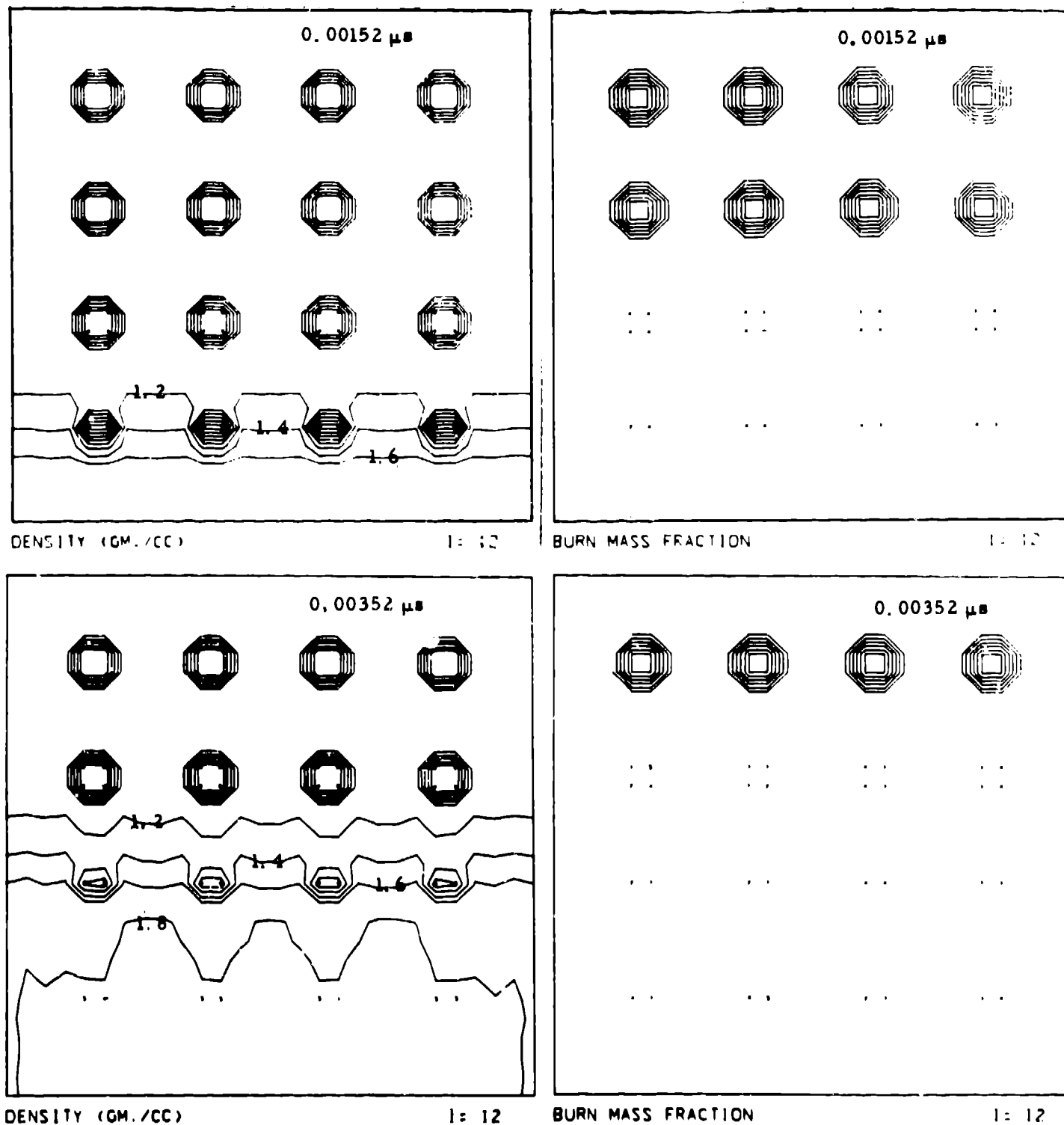
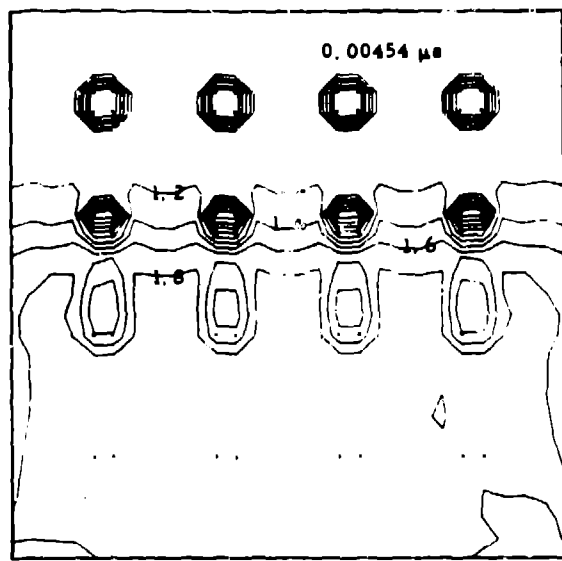
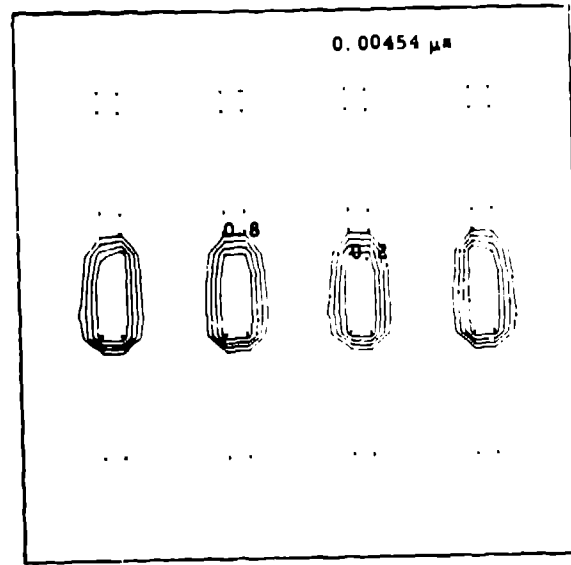


Fig. 5. The cross sections for the 12th cell in the x-direction for the interaction of a 5.5-GPa shock for  $1.6 \times 10^{-3} \mu s$  followed by an 8.5-GPa shock in a 0.028-mm cube of nitromethane with ninety-one 0.002-mm cubical holes. The interval between isopycnics is  $0.2 \text{ mg/mm}^3$  and between burn fraction is 0.2. Shows desensitization by preshocking.



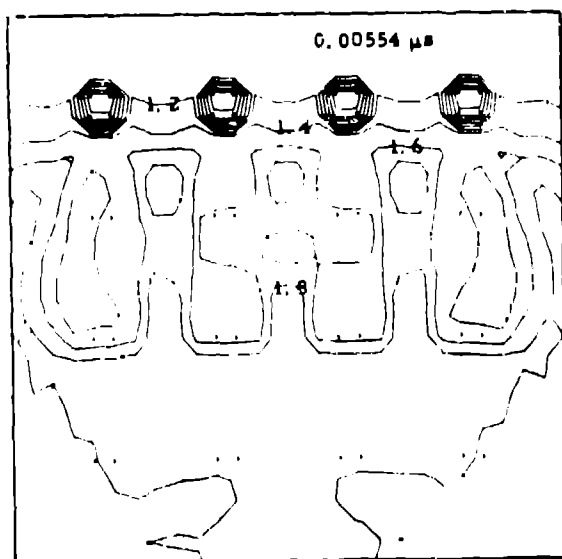
DENSITY (GM./CC)

1: 12



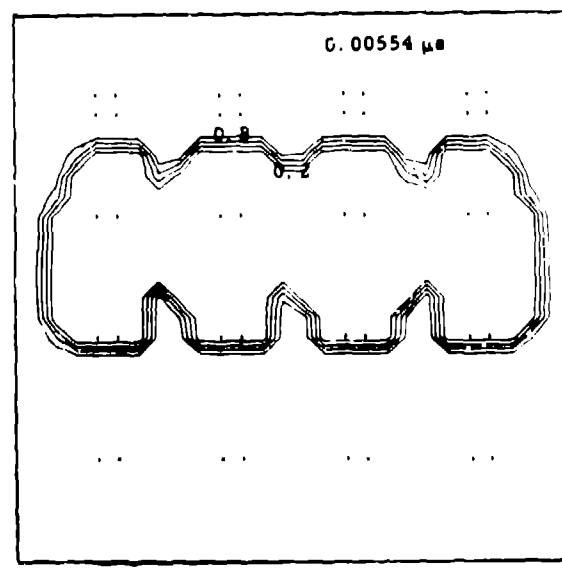
BURN MASS FRACTION

1: 12



DENSITY (GM./CC)

1: 12



BURN MASS FRACTION

1: 12

Fig. 5. (cont)

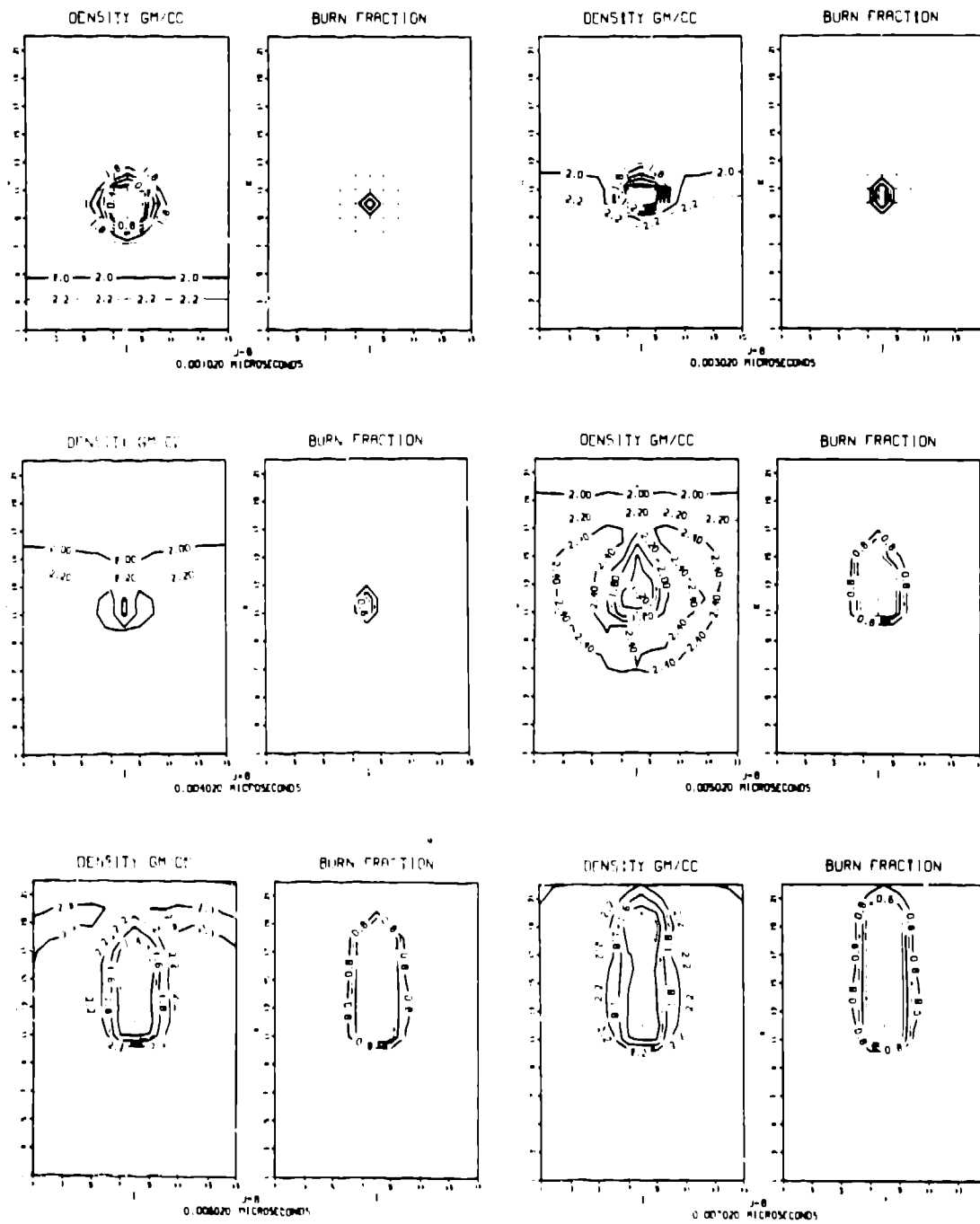


Fig. 6. A  $4 \times 10^{-3}$ -mm diameter spherical air hole in HMX. The initial shock pressure is 5.0 GPa. The density and burn fraction cross sections through the center of the hole are shown at various times. The flow does not build toward detonation.

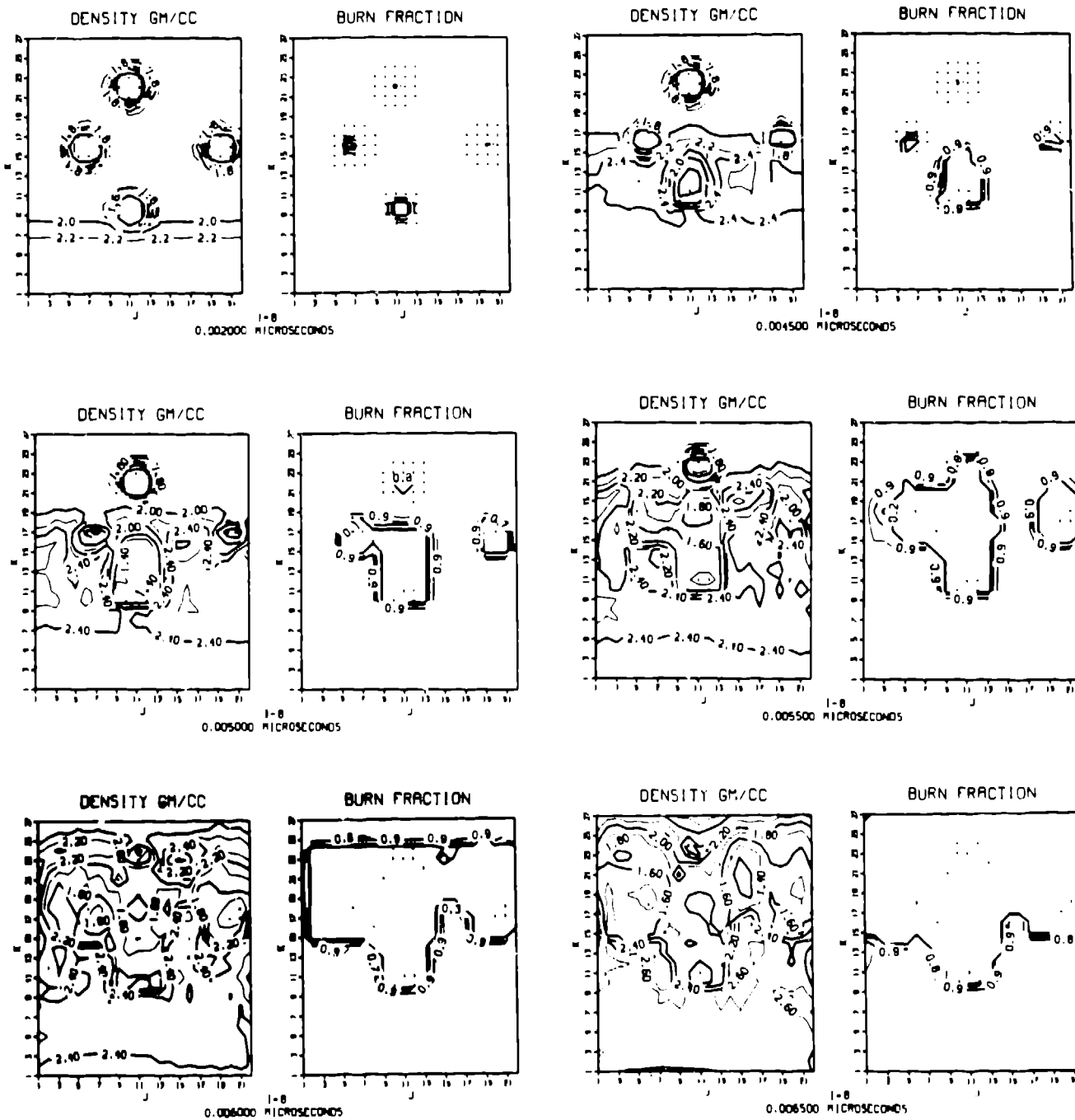


Fig. 7. A matrix of 10% air holes in HMX. The spherical air holes have a diameter of  $4 \times 10^{-3}$  mm. The initial shock pressure is 5.0 GPa. The density and mass fraction contours are shown for a cross section through the center of the matrix. The flow builds toward a propagating detonation.



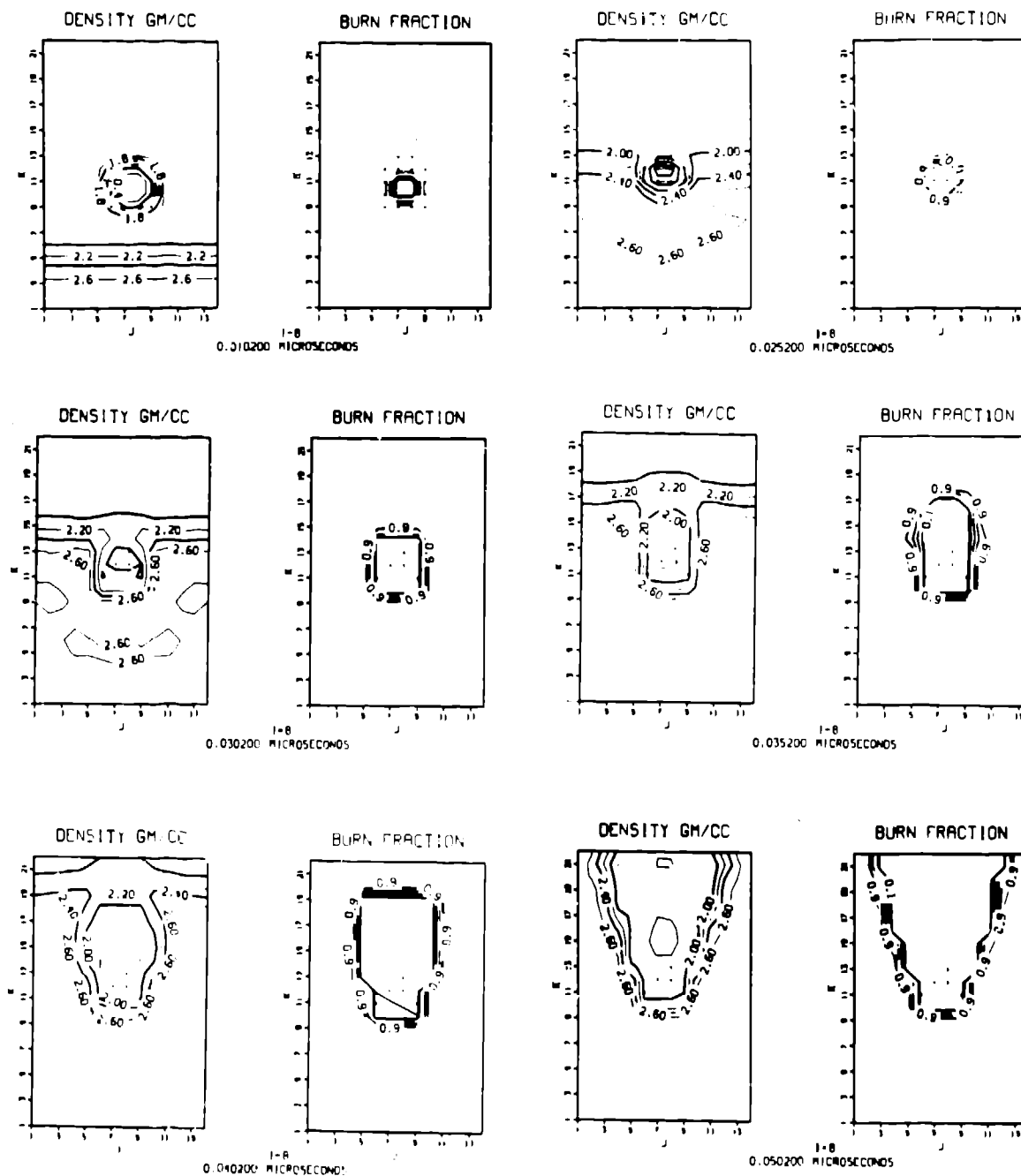


Fig. 8. A  $4 \times 10^{-3}$ -mm diameter spherical hole in TATB. The initial pressure is 12.5 GPa. The density and burn fraction cross sections through the center of the hole are shown at various times. The flow does not build toward a detonation.

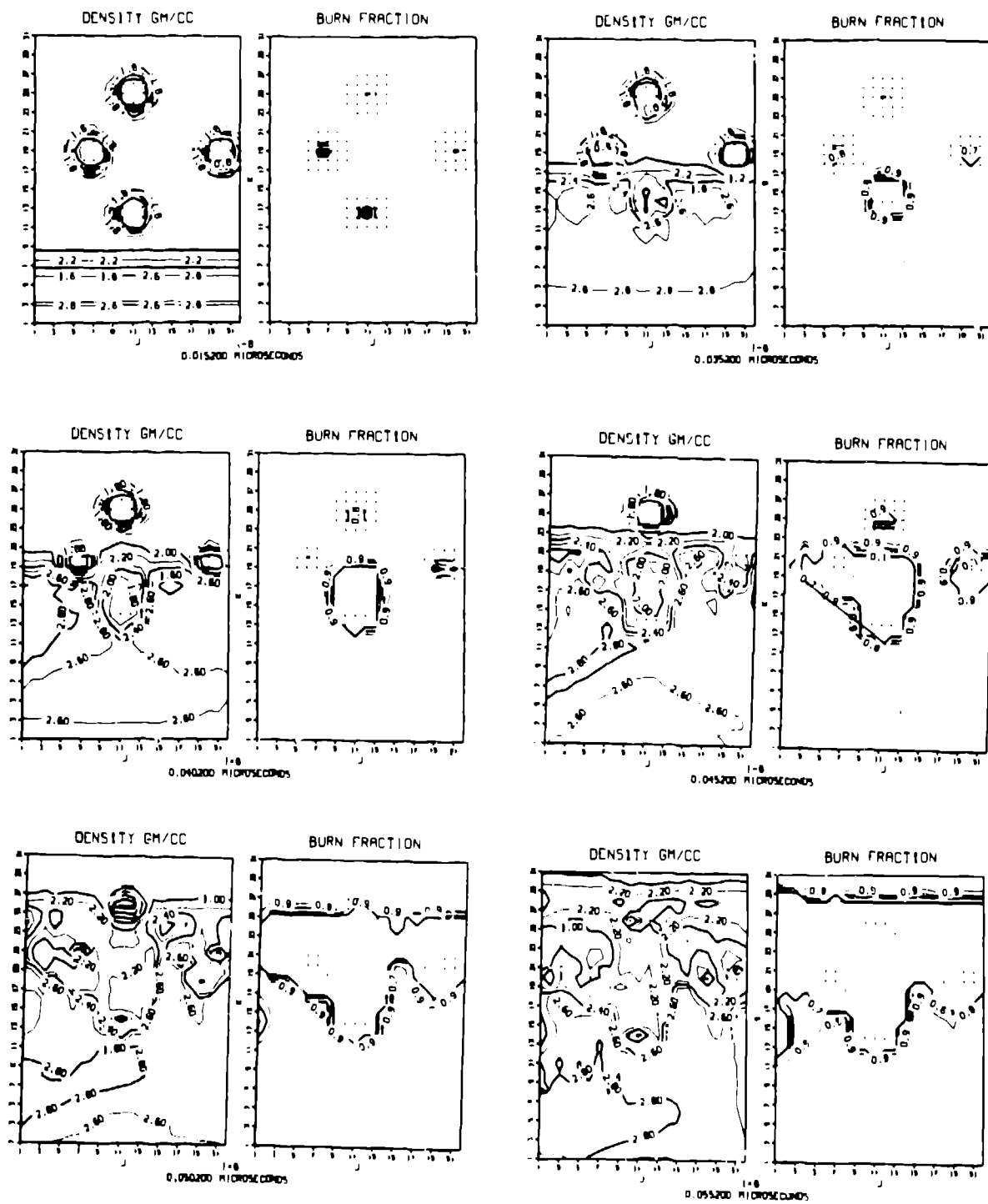


Fig. 9. A matrix of 10% air holes in TATR. The spherical air holes have a diameter of  $4 \times 10^{-3}$  mm. The initial shock pressure is 12.5 GPa. The density and mass fraction contours are shown for a cross section through the center of the matrix. The flow builds toward a detonation.

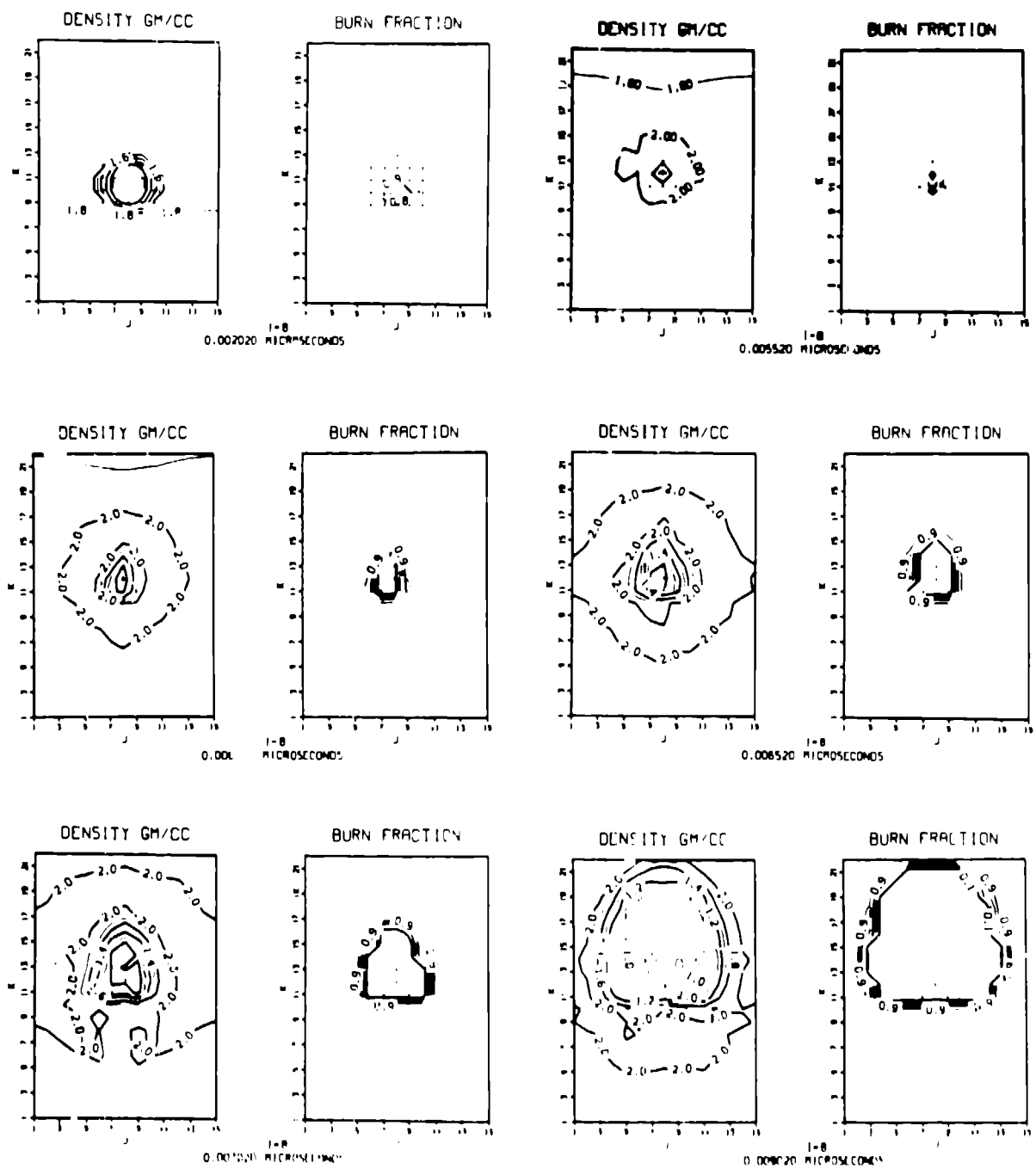


Fig. 10. A  $4 \times 10^{-3}$ -mm diameter spherical air hole in PETN. The initial shock pressure is 2.0 GPa. The density and burn fraction cross sections through the center of the hole are shown at various times. The flow does not build toward a detonation.

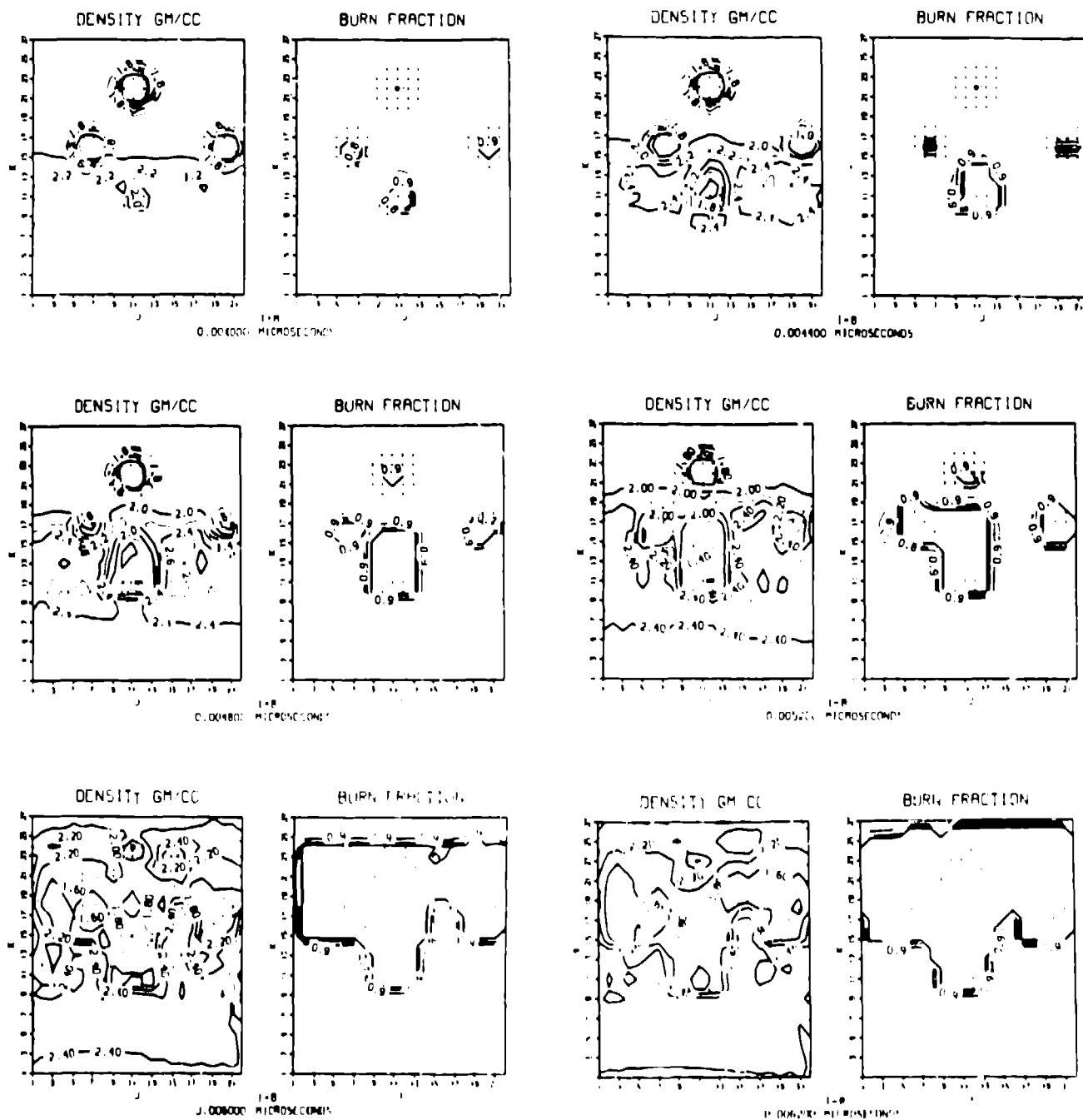


Fig. 11. A matrix of 10% air holes in PETN. The spherical air holes have a diameter of  $4 \times 10^{-3}$  m. The initial shock pressure is 2.0 GPa. The density and mass fraction contours are shown for a cross section through the center of the matrix. The flow builds toward a detonation.